Structure of $B_{13}C_2$

D. M. Bylander and Leonard Kleinman
Department of Physics, University of Texas, Austin, Texas 78712
(Received 8 June 1990)

By comparing calculated lattice constants with x-ray data as well as by comparison of calculated free energies, we find that the correct structure of $B_{13}C_2$ is B_{12}(CBC) rather than $B_{11}C$(BBC), as had been suggested. We also show that $B_{12}C_3$ is stable against $13B_{12}C_3 \rightarrow 12B_{13}C_2 + 15C$ as is $B_{13}C_2$ against $3B_{13}C_2 \rightarrow 2B_{12}C_3 + 15B$.

I. INTRODUCTION

This is the third paper of a series on boron and its carbides in which we calculate cohesive energies, heats of formation, energy bands, bond charge densities, lattice constants, and atomic positions within the unit cell from first principles. $B_{12}C_3$, B_{12}, and $B_{13}C_2$ all consist of a rhombohedral lattice of B_{12} or $B_{11}C$ icosahedra. The icosahedral top atoms in one plane each bond with a bottom icosahedral atom in the next plane, while in B_{12} each equatorial atom of an icosahedron forms a Δ bond with equatorial atoms from two other icosahedra. In the carbides this weak Δ bond is replaced by three bonds to an atom at the end of a three-atom interstitial chain. Unfortunately, x rays cannot distinguish between boron and carbon atoms so that there has always been uncertainty about whether the carbide icosahedra are B_{12} or $B_{11}C$. Although identical $B_{11}C$ icosahedra would destroy the rhombohedral symmetry of a perfect crystal, which x rays presumably would detect, at the high temperatures at which the carbides are made, the carbons are expected to occupy sites on the top and bottom triangles of the icosahedra in a random fashion, maintaining the overall rhombohedral symmetry. The general consensus[1–3] is that $B_{12}C_3$ has the $B_{11}C$(CBC) structure. Therefore it was gratifying to find in paper I (Ref. 4, hereafter called I), that $B_{11}C$(CBC) has 1.28 eV more binding energy per unit cell than B_{12} (CCC) as well as finding the calculated atomic positions of $B_{11}C$(CBC) in better agreement with the x-ray results than those of B_{12}(CCC). In paper II (Ref. 5, hereafter called II) we studied the energy bands and bonding of B_{12}. Because of the weakness of the in-plane Δ bonding, the calculated cohesive energy of B_{12} was 0.42 eV per atom less than that of $B_{11}C$(CBC).

There is no consensus regarding the $B_{13}C_2$ structure. Although unable to distinguish between B and C, x rays do show[3,6] that the icosahedron expands in going from $B_{12}C_3$ to $B_{13}C_2$ and then remains of constant size with further carbon depletion. Thus it is assumed that it is the carbon atom on the icosahedron that is initially being replaced and therefore the correct structure is B_{12}(CBC). On the other hand, Emin from analyses of free energy,[7] Raman spectra,[8] electron-spin resonance,[9] thermal conductivity,[10] and a theory of electronic conductivity and the Seebeck coefficient based on phonon-assisted bipolaron hopping[1] concludes that the structure is $B_{11}C$(BBC). In this work we find that B_{12}(CBC) has 2.09 eV more binding energy per unit cell and a free energy 1.67 eV more negative than $B_{11}C$(BBC). In addition, we find B_{12}(CBC) has lattice constants in much better agreement with the x-ray data. Also, in an attempt to understand why $B_{1-x}C_x$ remains stable in the same crystal structure with negligible interstitials[3] over the huge range $0.200 \leq x \leq 0.088$, we are able to show that

$$3B_{13}C_2 \rightarrow 2B_{12}C_3 + 15B \quad (1)$$

and

$$13B_{12}C_3 \rightarrow 12B_{13}C_2 + 15C \quad (2)$$

are energetically unfavorable. But, with the fairly gross assumption that the binding energy of $B_{1-x}C_x$ for $x < 2/15$ is an average of $B_{13}C_2$ and $B_{14}C_1$ binding energies, we find $B_{1-x}C_x$ is unstable for x infinitesimally less than 2/15. Thus the reason for the stability for $0.133 \leq x \leq 0.088$ remains a puzzle.

II. CALCULATIONS AND RESULTS

Our computational method is fully described in three appendixes to I. We sample the same quasi-fcc Brillouin zone (BZ) $(\frac{1}{4},\frac{1}{4},\frac{1}{4})$ and $(\frac{3}{4},\frac{1}{4},\frac{1}{4})$ special $\mathbf{k}$ points described in Appendix B. These 32 points reduce to 5 for B_{12}(CBC) and 10 for $B_{11}C$(BBC), which in the ordered crystal we assume for computational purposes has no threefold axis. Because $B_{13}C_2$ has a metallic band structure, we doubled the number of points sampled by including the 32 quasi-fcc reciprocal space cube-center points (0,0,0), $(\frac{1}{2},0,0)$, $(\frac{1}{2},\frac{1}{2},0)$, $(\frac{1}{2},\frac{1}{2},\frac{1}{2})$, (1,0,0) and $(1,\frac{1}{2},0)$, which increased the number of independent points to 13 for B_{12}(CBC). Because the energy gained by doubling the BZ sample was only 2 meV per atom for B_{12}(CBC), we did not double it for the less interesting $B_{11}C$(BBC). As with $B_{12}C_3$, we included all plane waves in our expansion with $(\mathbf{k}+\mathbf{G})^2 < 43.946$ Ry, which here required a maximum of 3718 plane waves.

The energy bands of the B_{12}(CBC) are displayed in Fig. 1. The symmetry points B, A, Z, and Γ are 0.372, 0.171, 0.157, and 0.121 eV above the Fermi energy, respectively. Above the twenty-fourth band the direct gaps at B, A, Z, and Γ are 3.390, 3.116, 3.396, and 5.301 eV with the indirect gap between B and A being 2.915 eV. These bands are very similar to those of $B_{11}C$(CBC) in I. If band structures were meaningful for these compounds, $B_{11}C$(CBC) would be a fairly wide-gap semiconductor and

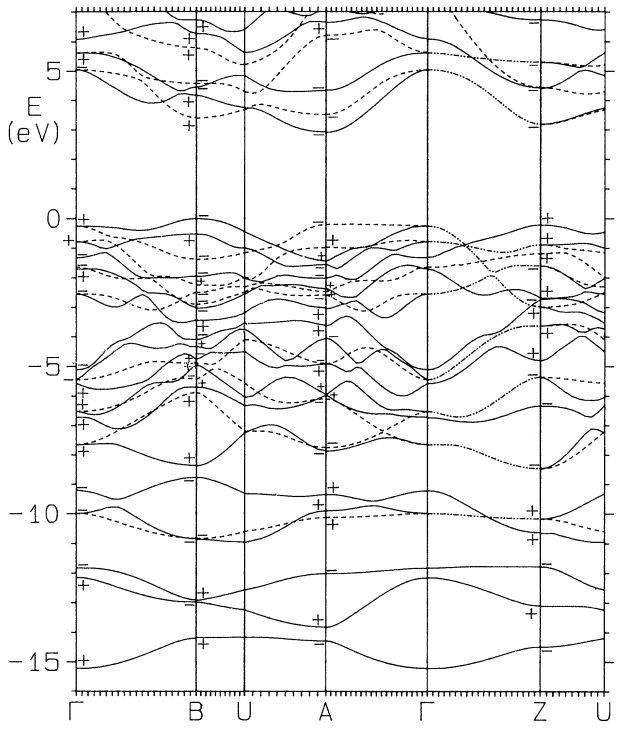

FIG. 1. Energy bands of $B_{13}C_2$. The solid (dashed) lines represent states that are even (odd) under reflection in a vertical plane. Along the threefold rotation axis from Γ to Z the dot-dashed lines represent twofold-degenerate states. The symmetry under inversion is shown by a + or − at symmetry points Γ, B, A, and Z. $\Gamma_1^{\pm}$ and $Z_2^{\pm}$ ($\Gamma_2^{\pm}$ and $Z_2^{\pm}$) become solid (dashed) lines in any direction, whereas $\Gamma_3^{\pm}$ and $Z_3^{\pm}$ states become either a dot-dashed line or a pair of lines, one solid and one dashed. The zero of energy is taken to be the top of the twenty-fourth band at B, which is 0.372 eV above the Fermi energy.

B_{12}(CBC) a metal. The analysis of Ref. 1 indicates that the conductivity in both $B_{12}C_3$ and $B_{13}C_2$ is due to hole hopping with an activation energy of only 0.14 eV but with the prefactor about seven times larger for $B_{13}C_2$. The larger conductivity of $B_{13}C_2$ is reasonable considering that its band structure requires one hole per unit cell but contradicts the older work of Samsonov quoted in Ref. 11 which finds that a plot of resistivity versus composition shows a series of maxima at $B_{12}C_3$,$B_{13}C_2$, and $B_{13}C$ with the $B_{13}C_2$ by far the most prominent. The fact that the conductivity shifts to lower values by as much as 30% with repeated thermal cycling[1] can be interpreted as implying that the perfect $B_{12}C_3$ crystal would be a wide-gap semiconductor and the perfect $B_{13}C_2$ crystal would be a Mott-Hubbard insulator.

In the first column of Table I we list our calculated cohesive energies[12] for B_{12}(CBC) and three different B_{11}C(BBC). If the chain carbon is assumed to be at one end of the chain, in the $\alpha(\gamma)$ structure the icosahedral carbon is in an equatorial site bonding to the other (same) end of the chain. See Fig. 1 of I. In the β structure the other carbon is in the far top or bottom icosahedral site, but since there is no C—C bond in either case, we will assume for the purpose of calculating the free energy that the near-top or bottom site gives the same cohesive energy. Thus there are six possible α arrangements, six γ's, and twelve β's. The free energy per 15-atom unit cell is (when only the mixing entropy is considered)

$$F(B_{11}C(BBC)) = -kT\ln(6e^{-15E_\alpha/kT} + 12e^{-15E_\beta/kT} + 6e^{-15E_\gamma/kT}), \quad (3)$$

whereas $F(B_{12}(CBC)) = -15E(B_{12}(CBC))$. Assuming that atomic interchanges cease below 2000 K and using the cohesive energies from Table I yields

$$F(B_{12}(CBC)) - F(B_{11}C(BBC)) = -1.669 \text{ eV/unit cell}. \quad (4)$$

Thus unless there is another contribution to the entropy that is vastly different for the two structures (such as a very soft BBC band of phonons), we must conclude that B_{12}(CBC) is the correct structure.

In Table II we list the lattice vectors and atomic positions of B_{12}(CBC) and the two most bound B_{11}C(BBC) structures. The z axis lies along the long diagonal of the reflection plane, i.e., the threefold axis for B_{12}(CBC). the y axis is perpendicular to the plane and the x axis is perpendicular to the y and z axes. The labeling of the atoms and lattice vectors is as in Fig. 1 of I. The icosahedral atoms also are labeled top (t), bottom ($\hat{t}$), and equatorial (e or $\hat{e}$) as in Fig. 1 of II. In Table III we compare the lattice constant, angle, and unit-cell volume of these structures with the x-ray results of Kirfel *et al.*[4] (KGW) as well as an average over two different crystals measured by Morosin *et al.*[13] The B_{11}C(BBC) calculated values a and α have been rhombohedrally averaged. The near-perfect agreement of the B_{12}(CBC) lattice constant with that of KGW must be considered somewhat fortuitous since in I and II the discrepancies between calculated and experimental values were only slightly less than $\frac{1}{2}$%, which is consistent with many other high-quality local-density-approximation calculations. On the other hand, the discrepancy between the calculated and experimental values of α is slightly larger for B_{12}(CBC) than those in I and II, but markedly smaller than those for either of the B_{11}C(BBC). Thus the x-ray data also strongly favor B_{12}(CBC) as the correct structure. In Table IV the seven different bondlengths of B_{12}(CBC) are compared with the experimental values. The agreement with the KGW results is excellent. By far the largest discrepancy occurs for the bond between a top atom in one icosahedron and a bottom atom in another; that discrepancy is only 0.546%. It should be noted that interpreting the atomic positions from x-ray data is not as clear cut as obtaining

TABLE I. Cohesive energy of B_{12}(CBC), B_{11}C(BBC) with three different positions of the icosahedral C, B_{12}(BBC), B_{11}C(CBC), B_{12}, and diamond in eV /atom.

$E(B_{12}(CBC))$	7.1408	$E(B_{12}(BBC))$	6.9312
$E(B_{11}C(BBC)_\alpha)$	7.0013	$E(B_{11}C(CBC))$	7.2592
$E(B_{11}C(BBC)_\beta)$	6.9926	$E(B_{12})$	6.8402
$E(B_{11}C(BBC)_\gamma)$	6.9482	E(C)	8.3895

TABLE II. Lattice vectors and atomic positions (in bohrs) for three different $B_{13}C_2$ structures in a Cartesian-coordinate system described in the text. The labeling of atoms and lattice vectors is that of Fig. 1 of I and Fig. 1 of II. The asterisks denote carbon atoms.

	B_{12}(CBC)	$B_{11}C(BBC)_\alpha$	$B_{11}C(BBC)_\beta$
$\overline{\theta\varphi}$	(6.1401,0,−7.6682)	(6.1225,0,−7.4026)	(6.0283,0,−7.4120
$\overline{\theta\psi}$	(−3.0700,−5.3175,−7.6682)	(−3.0613,−5.3683,−7.6688)	(−3.2014,−5.3670,−7.5587)
$\overline{\theta\omega}$	(−3.0700,5.3175,−7.6682)	(−3.0613,5.3683,−7.6688)	(−3.2014,5.3670,−7.5587)
B	(0,0,0)	(0,0,0)	(0,0,0)
C	(0,0,2.7252)*	(0.0401,0,2.7924)*	(0.0670,0,2.8047)*
K	(0,0,−2.7252)*	(−0.1605,0,−2.9611)	(−0.0662,0,−2.8937)
$\hat{t}z$	(1.9842,0,8.9084)	(2.1271,0,8.8080)	(2.1896,0,8.7081)
tc	(−1.9842,0,−8.9084)	(−2.0920,0,−8.8117)	(−2.1035,0,−8.7504)*
$\hat{t}x$	(−0.9921,1.7184,8.9084)	(−0.8751,1.7441,8.8213)	(−0.8502,1.7410,8.7516)
tb	(0.9921,−1.7184,−8.9084)	(0.8305,−1.7305,−8.7077	(0.8257,--1.7333,−8.6196)
$\hat{t}y$	(−0.9921,−1.7184,8.9084)	(−0.8751,−1.7441,8.8213)	(−0.8502,−1.7410,8.7516)
ta	(0.9921,1.7184,−8.9084)	(0.8305,1.7305,−8.7077)	(0.8257,1.7333,−8.6196)
ed	(−2.9989,0,−3.2490)	(−3.1709,0,−3.2563)*	(−3.1305,0,−3.1809)
$\hat{e}w$	(2.9989,0,3.2490)	(3.0266,0,3.3535)	(3.0603,0,3.3442)
eg	(1.4995,2.5972,−3.2490)	(1.4590,2.6977.−3.0686)	(1.4738,2.6820,−3.0344)
$\hat{e}k$	(−1.4995,−2.5972,3.2490)	(−1.4509,−2.6415,3.2428)	(−1.4431,−2.6409,3.2179)
eh	(1.4995,−2.5972,−3.2490)	(1.4590,−2.6977,−3.0686)	(1.4738,−2.6820,−3.0344)
$\hat{e}v$	(−1.4995,2.5972,3.2490)	(−1.4509,2.6415,3.2428)	(−1.4431,2.6409,3.2179)

the lattice vectors and that the discrepancies between the two sets of experimental results in Table IV are larger than those between the KGW results and our calculated values.

Because the icosahedral carbon atom in $B_{11}C$(CBC) appeared to hold its charge quite closely, we questioned in I whether the replacement of an icosahedral boron by a carbon enhanced the bonding. Taking 15 $[E(B_{11}C(CBC))-E(B_{12}(CBC))]$ from Table I, we see that in fact it enhances the cohesive energy by 1.78 eV. We may also compare its effect on heats of formation. We have $H(B_{13}C_2)=15E(B_{12}(CBC))-13E(B_{12})-2E(C)=1.41$eV, which is 0.22 eV less than the value of $H(B_{12}C_3)$ obtained in I. Thus 1.78 eV more energy is released in the formation of $B_{12}C_3$ compared to $B_{13}C_2$ if one begins with atomic constituents but only 0.22 eV if one starts with crystalline constituents. Nevertheless, $B_{13}C_2$ is thermally more stable. It is reported[11] to melt congruently at 2450 and 2480 °C while $B_{12}C_3$ melts incongruently at 2350 and 2360 °C. These results need not be contradictory if the excess cohesive energy and formation enthalpy of $B_{12}C_3$ arises from the Coulomb energy of electronic charge captured by icosahedral carbon at the expense of bonding charge.

The free energy per unit cell of $B_{12}C_3$ is $F(B_{12}C_3)=-15E(B_{11}C(CBC))-kT\ln 5=-109.1654$ eV, where we have accounted for five of the six t and $\hat{t}$ carbon sites that do not bond to another carbon. Although we have made no $B_{11}C$(CBC) calculations with carbon-carbon bonds, if we assume that the energy cost for either a t-$\hat{t}$ or an equatorial-chain carbon-carbon bond is equal to the difference in energy between the α and γ $B_{11}C$(BBC) structures, the contribution of these high-lying states to the free energy can be estimated. We find then that $F(B_{12}C_3)=-109.1677$ eV. On the other hand, $F(B_{13}C_2)=-15E(B_{12}(CBC))=-107.1120$ eV because the $B_{11}C$(BBC) lie so much higher in energy (less cohesive energy) as to have no contribution to the free energy. Inserting these values as well as E(C) and $E(B_{12})$ in Eqs. (1) and (2) we find $B_{13}C_2$ is stable against decomposing into $\frac{2}{3}B_{12}C_3+5B$ by 0.1325 eV, whereas $B_{12}C_3$ is stable against decomposition into $(12B_{13}C_2+15C)/13$ by 0.6149 eV. Thus the stability of $B_{1-x}C_x$ for $0.20\le x<0.1333$ is understandable. We have $F(B_{14}C)=-15E(B_{12}(BBC))-kT\ln 2=-104.0875$ eV. Therefore,

$$B_{14}C\rightarrow 14B+C+0.0648\text{ eV}, \tag{5}$$

$$B_{14}C\rightarrow \tfrac{1}{2}B_{13}C_2+\tfrac{15}{2}B+0.7700\text{ eV}, \tag{6}$$

and we see that for $x<0.1333$ $B_{1-x}C_x$ would be expected to phase separate into $B_{13}C_2$ and B. In fact, the addition-

TABLE III. Lattice constant, angle, and unit-cell volume for three $B_{13}C_2$ structures compared with the experimental values of KGW (Ref. 6) and MMES (Ref. 13).

	B_{12}(CBC)	$B^{11}C(BBC)_\alpha$	$B_{11}C(BBC)_\beta$	KGW	MMES
a (bohrs)	9.8235	9.768	9.723	9.823	9.801
α	65.544°	66.20°	66.73°	65.62°	65.605°
Ω (bohrs^3)	751.089	747.28	744.02	751.99	746.71

TABLE IV. Bond lengths of B_{12}(CBC) in bohrs compared with experimental values of KGW (Ref. 6) and MMES (Ref. 13). The first four bonds are intraicosahedral and the last three are intericosahedral, chain-icosahedral, and chain-chain, respectively. The number of equivalent bonds precedes the bond type.

	B_{12}(CBC)	KGW	MMES
$6e\hat{e}$	3.3520	3.3505	3.339
$6t\hat{e}$	3.3830	3.3883	3.392
$6te$	3.4068	3.4072	3.417
$6tt$	3.4368	3.4469	3.428
$3t\hat{t}$	3.2967	3.2787	3.252
$6eC$	3.0443	3.0557	3.042
$2CB$	2.7252	2.7174	2.714

al mixing entropy will allow a small amount of $B_{14}C$ to be mixed with $B_{13}C_2$ without phase separation. If we assume that the cohesive energy of the mixture is just that of the constituents, we calculate that at 2000 K the maximum number of $B_{14}C$ that can be mixed into $B_{13}C_2$ without the $B_{14}C$ phase separating is 1 in 2756. Thus the stability of $B_{1-x}C_x$ for $0.1333 < x < 0.088$ is not understood. We can only speculate that growth kinetics favors a huge number of imperfections in these crystals and that substituting a $B_{14}C$ for a unit cell with an imperfection in it is not so energetically unfavorable.

Contours of constant charge density in the reflection planes of B_{12}(CBC) are plotted in Fig. 2 and in the three independent faces of the icosahedron in Fig. 3. The boron atoms are centered in the small "40" contours and the carbons in the small "120" contours, which lie along the long diagonal of the reflection plane. The "120" contour along the top edge of Fig. 2 is an intericosahedral bond and the two small "120" contours on the line joining the boron in the edge to the one below the edge lie along the intraicosahedral t-$\hat{e}$ edge of Fig. 3. The icosahedral-chain bond is seen to peak at 280 millielect-

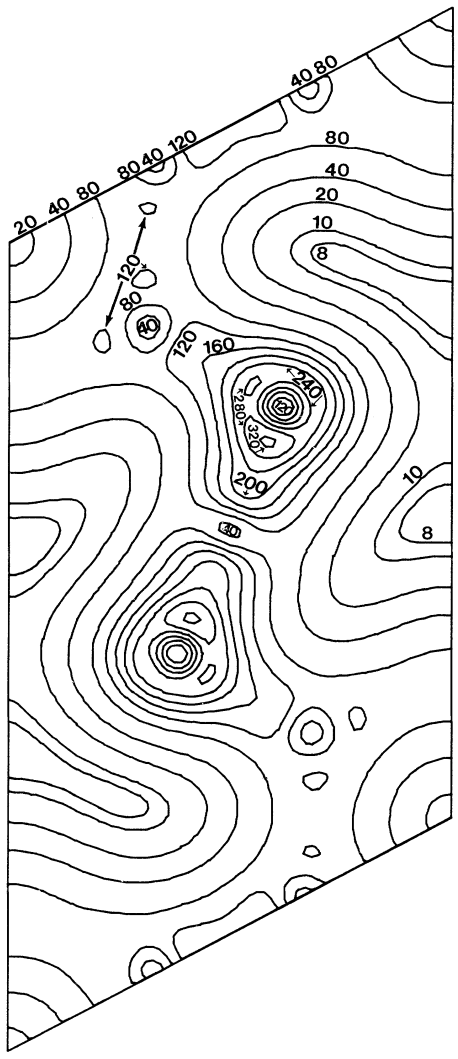

FIG. 2. Contours of constant charge density in the reflection plane. The contours, in units of millielectrons per cubic bohr, are 8, 10, 20, 40, and then increasing in steps of 40.

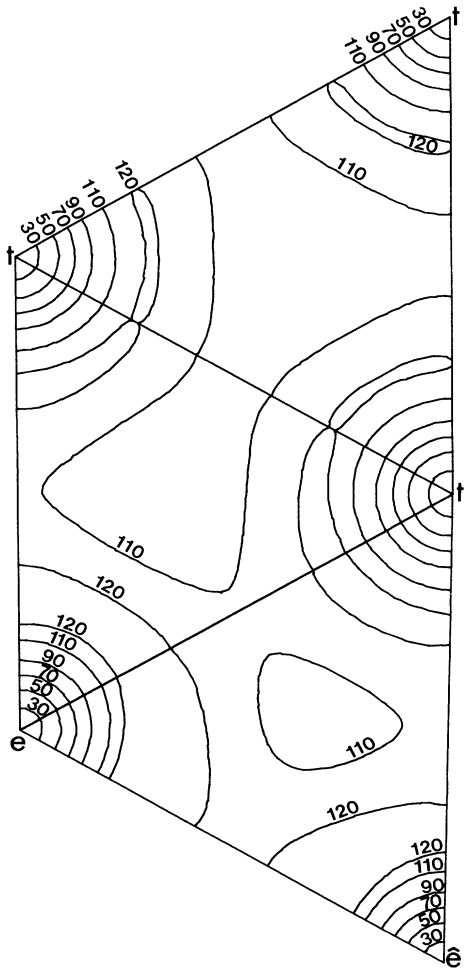

FIG. 3. Contours of constant charge density in the three independent icosahedral faces. The contours plotted are 30, 50, 70, 90, 110, and 120 millielectrons per cubic bohr.

rons per cubic bohr and the chain-chain bond at 320. The boron-boron and two boron-carbon bonds just mentioned all have the same peak contours as we found in I for $B_{11}C$(CBC). Thus the replacement of the icosahedral carbon by a boron has only a small effect on bonds not involving that atom. We will not discuss the contributions of individual eigenstates to the bonding as we did in I and II; Switendick[14] has discussed this for B_{12}(CBC). We note only that the ordering of the states contributing to various bonds is different at different points in the BZ and that at Z, unlike Γ and B, the states at the top of the valence band are diffuse and cannot be characterized as contributing strongly to any bond.

In conclusion, we have shown by both free-energy calculations and a comparison with x-ray data that $B_{13}C_2$ has the B_{12}(CBC) and not the $B_{11}C$(BBC) structure, as had been suggested.[1,7–10] We have also shown that $B_{13}C_2$ and $B_{12}C_3$ are both energetically stable, but that $B_{13}C_{2-x}$ should phase separate into $B_{13}C_2$ and boron. The fact that $B_{13}C_{2-x}$ exists for x as large as 0.74 we attribute to the growth kinetics of the sintering process.

ACKNOWLEDGMENTS

This work was supported by the Robert A. Welch Foundation (Houston, Texas), the University of Texas Center for High Performance Computing, the Texas Advanced Research Program, and the National Science Foundation under Grants No. DMR-8718048 and No. 9015222.

[1]Charles Wood and David Emin, Phys. Rev. B **29**, 4582 (1985).

[2]M. Van Schilgaarde and W. A. Harrison, J. Chem. Phys. Solids **46**, 1093 (1985).

[3]A. C. Larson, in *Boron Rich Solids,* AIP Conf. Proc. No. 140, edited by D. Emin, T. Aslage, C. L. Beckel, I. A. Howard, and C. Wood (AIP, New York, 1986). p. 109.

[4]D. M. Bylander, Leonard Kleinman, and Seongbok Lee, Phys. Rev. B **42**, 1394 (1990).

[5]Seongbok Lee, D. M. Bylander, and Leonard Kleinman, Phys. Rev. B **42**, 1316 (1990).

[6]A. Kirfel, A. Gupta, and G. Will, Acta. Crystallogr. B **35**, 1052 (1979).

[7]D. Emin, Phys. Rev. B **38**, 6041 (1988).

[8]D. R. Tallant, T. S. Aselage, A. N. Campbell, and D. Emin, Phys. Rev. B **40**, 5649 (1989).

[9]E. L. Venturini, D. Emin, and T. L. Aselage, in *Novel Refractory Semiconductors,* edited by D. Emin, T. L. Aselage, and C. Wood (Materials Research Society, Pittsburgh, 1987), p. 83.

[10]D. Emin, I. A. Howard, T. A. Green, and C. L. Beckel, in Ref. 9, p. 83.

[11]J. L. Hoard and R. E. Hughes, in *The Chemistry of Boron and Its Compounds,* edited by E. L. Muetteries (Wiley, New York, 1967), p. 25.

[12]The boron and carbon atomic energies that are subtracted from the binding energy to obtain the cohesive energy cancel out when comparing different $B_{13}C_2$ structures; they also cancel in reaction equations such as (1) and (2). We noted in II that the errors in the B and C atomic energies are almost identical, so that comparisons of the $B_{13}C_2$ and $B_{12}C_3$ cohesive energies also are meaningful.

[13]B. Morosin, A. W. Mullendore, D. Emin, and G. A. Slack, in Ref. 3, p. 70.

[14]A. C. Switendick, in *Proceedings of NATO Advanced Research Workshop on the Physics and Chemistry of Carbides, Nitrides, and Borides, Manchester, England, 1989,* Vol. 185 of *NATO Advanced Study Institute Series E: Applied Sciences,* edited by Robert Freer (Kluwer, Dordrecht, 1990).